Structural and electronic properties of cubic, 2H, 4H, and 6H SiC

C. H. Park,* Byoung-Ho Cheong, Keun-Ho Lee, and K. J. Chang
Department of Physics, Korea Advanced Institute of Science and Technology, 373-1 Kusung-dong, Yusung-ku, Daejon, Korea
(Received 30 August 1993; revised manuscript received 13 October 1993)

We study the structural and electronic properties of various polytypes of SiC through self-consistent *ab initio* pseudopotential calculations. For the wurtzite (2*H*), 4*H*, and 6*H* structures, the equilibrium lattice constants and bulk moduli are very similar to those for the cubic structure. The energies calculated for the polytypes considered here are very close to within 4.3 meV/atom, which may explain the polytypism of SiC. The 4*H* structure is found to be lowest in energy because of the attractive interactions between the alternating cubic and hexagonal stacking layers, while the wurtzite structure is most unstable among the polytypes. We find the asymmetric charge distribution for a Si-C bond to be on the boundary separating the zinc-blende and wurtzite phases, which should be related to the polytypism of SiC. In the hexagonal polytypes, the *M* conduction-band energy increases, while that of the *K* point decreases as the hexagonal close packing becomes more prominent. Thus, the conduction-band minimum state located at the *X* point for cubic SiC changes to the *M* point, and then to the *K* point for the 2*H* structure. For the cubic structure, the density of states near the conduction-band edge increases slowly with energy, while it shows very rapidly increasing behavior for the 6*H* polytype because its conduction-band edge states are flattened due to the band folding and the energy-increasing behavior of the *M* state when the hexagonal-close-packing nature is enhanced.

I. INTRODUCTION

SiC crystallizes in either a cubic or a hexagonal form, and exhibits polytypism.[1,2] The polytypes consist of identical layers, whose stacking sequences differ, and can be considered as natural superlattices. Although several theoretical studies have been performed,[3–6] the origin of the polytypism is still the subject of many investigations. The SiC polytypes are semiconductors with a wide range of band gaps, varying from 2.39 eV in the zinc-blende structure (3*C* SiC) to 3.33 eV in the wurtzite polytype (2*H* SiC).[1,7] Among many polytypes, 3*C* and 6*H* SiC are of great interest because these materials are used for the fabrication of electronic devices; 3*C* SiC is used for high-temperature, high-power, and high-frequency operation of devices, while 6*H* SiC with a band gap of 2.86 eV is a promising material for blue light-emitting-diode applications.[7] The strong bonding between the Si and C atoms in SiC makes this material highly resistant to high temperature and radiation, and thus causes low diffusion rates for both dopant and host atoms. Moreover, *p*- and *n*-type dopings have been shown to be easier, compared with other wide-band-gap materials such as ZnS, ZnSe, and GaN.[7] In spite of such unique properties of SiC, electronic-device applications have been delayed. In recent years, with the development of crystal-growing techniques, interest in SiC and its device applications has been growing rapidly.[7]

To understand the polytypism, it is important to examine the structural properties of the polytypes of SiC. Recently, the first-principles local-density-functional technique has been applied for studying the ground-state properties of the cubic[8–13] and 2*H* polytypes of SiC.[11,12] Those calculations were not performed for the 4*H* and 6*H* structures. From extensive pseudopotential calculations, Heine and co-workers investigated the interaction energies between the SiC double layers to examine SiC polytypism.[3–6] The energy band structure and the elastic properties of SiC in the 3*C* structure have been calculated by several groups.[8,13,14] Calculations using linear combination of atomic orbitals for 2*H* SiC showed valence-band features which agree with experiment, but unrealistic conduction bands were obtained due to the restriction to nearest-neighbor interactions in the Hamiltonian matrix.[15] Recently, a first-principles linear muffin-tin orbital (LMTO) method was used to study the energy-band structures and optical properties of 2*H*, 4*H*, and 6*H* SiC.[16]

In this paper, we present the results of *ab initio* pseudopotential calculations for studying the ground-state properties of SiC in the 3*C*, 2*H*, 4*H*, and 6*H* structures. These include the zero-pressure lattice constants, bulk moduli, and total energies. The stability of the polytypes is found to be strongly related to the hexagonal-close-packing nature, and the 4*H* structure with alternating cubic and hexagonal stacking layers is found to be most stable among the polytypes. The energy-band structures and deformation potentials of the direct and indirect band gaps for the polytypes are also calculated and compared with available experimental data and other calculations. As the hexagonal stacking nature becomes more prominent, the polytypes show significant changes in the conduction band; the energy of the lowest conduction-band state at the *M* point is found to increase, while the *K* conduction-band state shows the opposite behavior. Thus, the lowest Γ-*X* gap in the cubic structure changes to the Γ-*M* indirect gap in the 4*H* and 6*H* structures, while for the 2*H* polytype with purely hexagonal stacking layers the lowest conduction-band state occurs at the *K* point. Moreover, the conduction-band edge states for the

0163-1829/94/49(7)/4485(9)/$06.00 ©1994 The American Physical Society

6*H* polytype with a large unit cell are nearly flattened due to large band foldings; thus, its density of states near the conduction-band threshold shows rapidly increasing behavior, compared with other hexagonal polytypes. In Sec. II we describe the method of calculation. In Sec. III the structural properties are presented and discussed. In Sec. IV the results of the calculations for the energy-band structure and the density of states are given and discussed with relation to other theoretical and experimental results. We summarize the results in Sec. V.

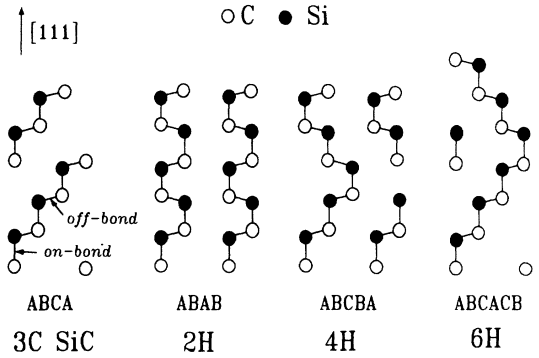

FIG. 1. Atomic structures of the polytypes of SiC are described in the hexagonal $(10\bar{1}0)$ plane. *A*, *B*, and *C* denote the type of atomic layer. The bonds aligned along the cubic [111] axis are denoted as on-bonds while the sidewise bonds are denoted as off-bonds.

II. METHOD

In our calculations we use the self-consistent total-energy pseudopotential method[17,18] within the local-density-functional approximation (LDA).[19] The exchange-correlation contribution to the total energy is described by the Wigner interpolation formula.[20] For the C atom, the 2*p* orbital is strongly localized because of the lack of *p* core states, and thus a large number of plane waves are required to achieve a high degree of accuracy. Norm-conserving nonlocal soft pseudopotentials for Si and C atoms are generated by the scheme proposed by Troullier and Martins,[21] then the Kleinman-Bylander type of fully separable pseudopotentials are constructed.[22] Since the *p* pseudopotential of carbon is very deep, controlling this potential is the main factor in achieving total-energy convergence. In the present calculations for SiC, we use the kinetic-energy cutoff ($E_{p\omega}$) of 50 Ry in the plane-wave expansion of the wave functions. As we increase $E_{p\omega}$ to 100 Ry, the change in total energy is less than 20 meV/atom. For 6*H* SiC, the matrix size is found to be about 5000 for the equilibrium volume. To diagonalize such an extremely large Hamiltonian matrix, an efficient iterative diagonalization method which was recently developed by us is employed.[23]

To see the energies, we examine the cubic and hexagonal (2*H*, 4*H*, and 6*H*) polytypes. Since these polytypes have tetrahedral bonds, their local atomic arrangements are the same up to the second neighbor. The structural difference in the polytypes is well understood by considering the stacking sequence of the cubic (111) or hexagonal (0001) planes.[1,2] All the structures consist of pairs of Si and C layers with successive pairs displaced sidewise (each pair is designated by *A*, *B*, or *C* in Fig. 1). In 3*C* SiC, every fourth stacking layer is positioned on top, giving rise to the stacking sequence *ABCABC*..., as seen in Fig. 1. The stacking sequence of the 2*H* structure is of the type *ABAB*..., while *ABCB*... and *ABCACB*... are the sequences for the 4*H* and 6*H* structures, respectively. Assuming that the 3*C* and 2*H* structures are extremes in the parameter describing the percentage of hexagonal close packing (often called "hexagonality[1]") with 0 and 100% respectively, we get the hexagonal nature of 50% for the 4*H* structure and about 33% for the 6*H* structure, examining the hexagonal stacking for individual layers. The periodic supercells for the 2*H*, 4*H*, and 6*H* structures contain four, eight, and twelve atoms, respectively.

The summation of the charge density over the irreducible Brillouin zone (BZ) is performed using a set of equivalent *k* points. For the cubic structure, we use a supercell containing six atoms, whose atomic layers are stacked along the cubic [111] direction, to compare its energy with those for the 2*H* and 6*H* structures. In this case, we choose 10 *k* points in the irreducible BZ, uniformly divided by four cuts along the Γ-*M* direction in the hexagonal BZ and two cuts along the Γ-*A* direction. When we test the case of the BZ divided by five cuts along the Γ-*M* direction (corresponding to 15 *k* points for the cubic structure), the change of the total-energy difference between the 2*H* and 3*C* structures is found to be only 0.2 meV/atom. The equivalent sets of *k* points for the 2*H* and 6*H* structures are generated by three cuts and one cut, respectively, along the Γ-*A* direction with the same grids in the hexagonal plane, resulting in 12 and 6 *k* points. For the 4*H* structure, we generate the equivalent set of *k* points to compare with the 2*H* structure by cutting twice less the Γ-*A* axis. This choice of the equivalent sets of *k* points ensures consistency in the comparison of the total energies for all the polytypes.

The density of states (DOS) is calculated by the linear-tetrahedron method over mesh points.[24,25] For the cubic structure, we generate 480 *k* points in the irreducible BZ, while for the hexagonal polytypes the numbers of *k* points are chosen to be 550, 280, and 224 for the 2*H*, 4*H* and 6*H* structures, respectively.

III. STRUCTURAL PROPERTIES

For the hexagonal polytypes, the lattice parameters (*a*, *c*, and internal parameter *u*) are all determined by minimizing crystal total energy. In this case, the internal atomic positions are fully relaxed by calculating the Hellmann-Feynman forces for a given volume.[26] The total-energy calculations are repeated for different *c*/*a* ratios with the same volume. With the *c*/*a* ratio fixed, then we determine the energy-versus-volume curve for each hexagonal polytype. The equilibrium lattice constant *a*, the bulk modulus B_0, and its first-order pressure

derivative B_0' are determined by fitting the volume-dependent total energies to the Murnaghan equation.[27]

The calculated values for a, B_0, and B_0' in the present study are shown in Table I and compared with other calculations[8-12,28,29] and experiments[1] C, Si, and SiC. The lattice constants and bulk moduli are in good agreement with available experimental data to within 0.6% and 10%, respectively, while the calculated axial ratios in the hexagonal polytypes are slightly larger than the ideal value, in good agreement with measured values to within 0.6%. For lattice parameters, we should mention that from previous experience on other materials, the Wigner formula constructed *ad hoc* for the exchange-correlation energy produces better agreement with experiment, while predictions coming from an exchange-correlation formula with more theoretical justification based on Ceperly and Alder data[30] usually underestimate the lattice parameters.[31] In Table I, we find here that for cubic SiC the Ceperly-Alder correlation gives a lattice constant which is smaller by 0.004 Å. For the 4*H* and 6*H* structures, neither experimental nor theoretical results for B_0 and B_0' are available. However, our calculations show that independently of the structure the polytypes of SiC have similar lattice constants, bulk moduli, and axial ratios. The lattice constant of 3*C* SiC is smaller by 0.138 Å than the average of those for Si and C. This reduction of the lattice constant results from charge transfer from the Si atom to the C atom, arising from the strong 2*p* potential of C when the Si-C bond is formed. The value for B_0 in 3*C* SiC is also 19% smaller than the average (2.71 Mbar) of the measured bulk moduli for C and Si. We estimate a value of B_0' ranging from 3.2 to 4.2 for the hexagonal polytypes of SiC, but experimental data are not available.

We find the 4*H* structure to be the most stable at zero temperature. The calculated total energies for the four structures are found to be in the order of $E_{2H} > E_{3C} > E_{6H} > E_{4H}$. Considering only the Ewald energy, which is the structure-dependent energy related to the ion-ion interactions, we find a preference for the cubic structure because the total energies are then in the order $E_{3C} < E_{6H} < E_{4H} < E_{2H}$ as the hexagonal stacking nature becomes more prominent. The same trend for the Ewald energy was also suggested in Ref. 11. Our calculated total energies for the 6*H*, 4*H*, and 2*H* structures relative to that of the 3*C* structure are −1.8, −2.5, and 1.8 meV/atom, respectively, as shown in Fig. 2. Previous calculations also showed that the energy differences between the polytypes are extremely small, of the order of meV/atom.[3-6] When we test the ideal hexagonal structures with no internal relaxations and ideal c/a ratios, we

TABLE I. Calculated lattice constants, bulk moduli, and bulk-modulus pressure derivatives for Si, C, and SiC. The 3*C*, 2*H*, 4*H*, and 6*H* polytypes are considered for SiC. For Si, C, and 3*C*, SiC, a denotes the cubic dimension. For cubic SiC, the results from the Ceperly-Alder correlation are given in parentheses.

	a (Å)	c/a	B_0 (Mbar)	B_0'
		Si		
Present	5.432		0.89	3.5
Other	5.433,[a] 5.435[b]		0.92[a,b]	3.6,[a] 3.56,[b]
Expt.[c]	5.429		0.99	4.2
		C		
Present	3.560		4.31	3.7
Other	3.561,[a] 3.607[b]		4.38,[a] 5.17[b]	3.5,[a] 2.5[b]
Expt.[c]	3.567		4.43	4.0
		3*C* SiC		
Present	4.358 (4.354)		2.19 (2.20)	3.3 (3.3)
Other	4.361,[a,d] 4.326,[e] 4.365[f]		2.12,[a,d] 2.50,[e] 2.00[f]	3.7,[a,d] 3.2,[e] 7.3[f]
Expt.[c]	4.360		2.24	
		2*H* SiC		
Present	3.072	1.641	2.152	4.2
Other[g]	3.120	1.611	2.16	
Expt.	3.076[b]	1.641[b]	2.23,2.25[h]	
		4*H* SiC		
Present	3.069	3.292	2.18	3.8
Expt.[b]	3.073	3.271		
		6*H* SiC		
Present	3.077	4.910	2.04	3.2
Expt.[b]	3.073	4.907		

[a] Reference 8 ($E_{p\omega}$=20 Ry for Si and 60 Ry for C).
[b] Reference 28 ($E_{p\omega}$=15 Ry for Si and 41 Ry for C).
[c] Reference 1.
[d] Reference 9 ($E_{p\omega}$ = 60 Ry).
[e] Reference 10 ($E_{p\omega}$ = 32 and 72 Ry using Lowdin perturbation).
[f] Reference 11 ($E_{p\omega}$ = 29.7 Ry).
[g] Reference 12 ($E_{p\omega}$ = 23.3 Ry).
[h] Reference 29.

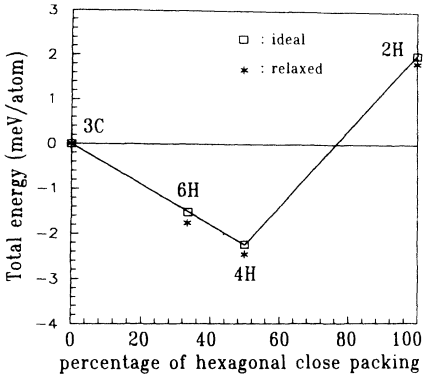

FIG. 2. Crystal total energies of the SiC polytypes relative to that of the 3*C* structure are plotted as a function of the parameter describing the percentage of hexagonal close packing.

find no change in the order of stability, with the corresponding energy differences −1.5, −2.3, and 2.0 meV/atom. In previous pseudopotential calculations,[8] the cubic structure was shown to be more stable by about 3 meV/atom than the 2*H* structure, in good agreement with the present result. The cohesiveness of SiC mainly results from the strong bonding between the adjacent Si and C atoms; thus, it costs an extremely low energy to change the sequence of the stacking layers. In fact, the calculated total energies for the polytypes are so close (to within 4.3 meV/atom) that the stability of the polytypes may be significantly affected by temperature and crystal-growing conditions.

For the 4*H* structure, the lattice consists of two different regions with alternating hexagonal and cubic stacking layers. In a hexagonal stacking layer, the off-axis bonds as shown in Fig. 1 face each other along the hexagonal direction. Then, the overlapping of the charge densities between the two off-bonds induces charge transfer into the neighboring cubic stacking layers. Figure 3 shows the planar-averaged charge densities $\Delta\bar{\rho}$ for the 2*H*, 4*H*, and 6*H* structures, which are subtracted from the charge density of the 3*C* structure, along the hexagonal axis. The $\Delta\bar{\rho}$'s are found to be very small, within 1% of the maximum charge density in the 3*C* structure. This small difference in charge density reflects the small difference of the total energies between the polytypes. We see clearly that the hexagonal layers of 4*H* SiC become slightly positively charged, while the cubic layers are negatively charged. Since the energy lowering due to the attractive interactions between the charged layers is largest for the 4*H* structure, this hexagonal structure has a minimum total energy. However, in the 2*H* structure, since each stacking layer has hexagonal bonding character, the charge overlap between the neighboring off-bonds is maximized. Thus, because of the resulting repulsive interactions, the 2*H* structure is highest in total energy and the c/a ratio is largest among the hexagonal polytypes.

The calculated valence charge densities $\rho(\mathbf{r})$ for 3*C*, 2*H*, 4*H*, and 6*H* SiC are plotted on the hexagonal $(10\bar{1}0)$ planes in Fig. 4. We find the charge densities to be simi-

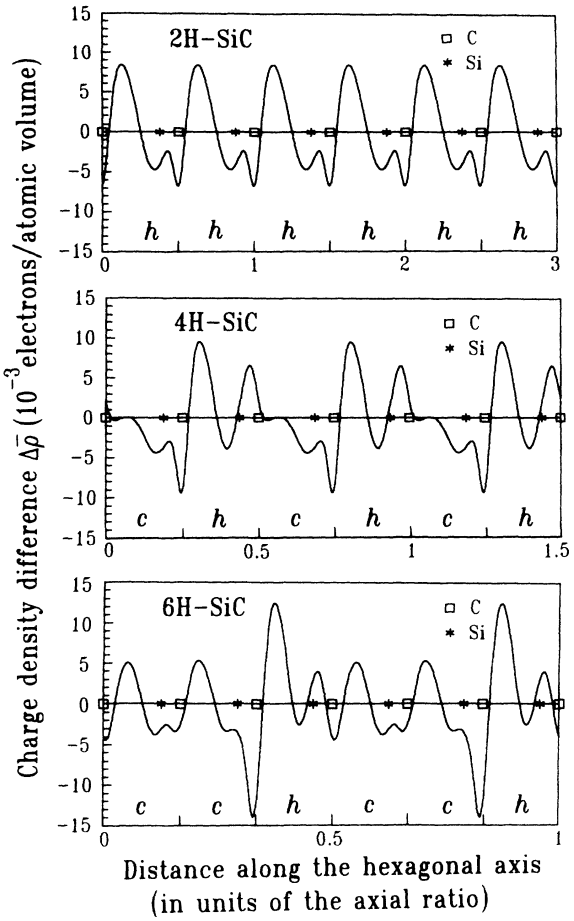

FIG. 3. Planar-averaged total valance charge densities $\Delta\bar{\rho}$ which are subtracted from that of the cubic structure are plotted along the hexagonal axis. *h* and *c* denote the hexagonal and cubic stacking layers, respectively.

larly distributed around the Si and C atoms, displaying features typical of ionic bonding. Because of the strong 2*p* potential of C, the charge density is strongly accumulated around the C atom, resulting in a large asymmetry in charge distribution. The charge asymmetry of a bond is very useful to understand the structural properties of SiC, such as the polytypism and the smaller lattice constant for cubic SiC than the average of those for Si and C. Recently, Garcia and Cohen made a direct connection between the valence charge distribution and the ionicity of a compound, and suggested the asymmetry of the charge density as a measure of the ionic character of a bond.[32] They established an unambiguous procedure to compute numerical values for the charge-asymmetry coefficient g and showed that there is a correspondence between g and the Phillips' ionicity f_i for many compound materials, except for SiC and BN which contain first-row elements. Although the Phillips' scale fails to account for some structural trends of materials containing first-row elements,[33] if the charge-asymmetry coefficient g is used instead of f_i, many basic properties of molecules and solids including first-row elements were shown to be successfully described.

Figure 5 shows the c/a ratio of the hexagonal struc-

ture versus the asymmetry coefficient g for many compounds, including SiC and BN. The compounds indicated by □ are known to show polytypism, as in SiC. We find a tendency that, if g is roughly above 0.5, the wurtzite structure is preferred over the zinc-blende structure. Then, the c/a ratio of this hexagonal structure is generally smaller than the ideal value of 1.633. Since g is proportional to f_i, the cation-anion bond with a large g value possesses more ionic character. The zinc-blende and wurtzite structures have similar tetrahedral bonds up to the second neighbor, and the local atomic arrangements which differ in the third neighbor are mapped upon each other by rotation over π around the bond axes. Thus, the anion atom in the wurtzite structure is more closely bonded to the third-neighbor cation, which is placed in the adjacent stacking layer right on top (see Fig. 1), resulting in more attractive interaction between the anion and cation atoms, as compared to the zinc-blende structure. Since such attractive interactions are enhanced for highly ionic systems, i.e., for larger g values, the wurtzite structure is stabilized against the zinc-blende structure. In this case, the layer spacings are reduced by the attractive interactions between the first and third layers with different charge states, and thus the c/a ratio is smaller than the ideal value. If g is less than 0.5, the attractive force discussed above is much reduced for the wurtzite structure, while the repulsive interactions due to charge overlap in the region between the anion and the third-neighboring cation increases the energy of the wurtzite structure. Thus, the zinc-blende structure is stabilized for systems with small g values. We find that the g values in SiC and BN are in the intermediate range around 0.5 separating the zinc-blende and wurtzite structures. A similar classification of SiC crystal has also been made based on bond-orbital coordinates r_σ and r_π.[34] As discussed earlier, the wurtzite structure of SiC is less stable by 1.8 meV/atom than the zinc-blende structure; thus its axial ratio is slightly larger than those for other compounds with the hexagonal structure. From these results we conclude that the polytypism of SiC along with that of BN should be related to the unique behavior of bond charge asymmetry and the closeness of the total energies between the cubic and hexagonal polytypes.

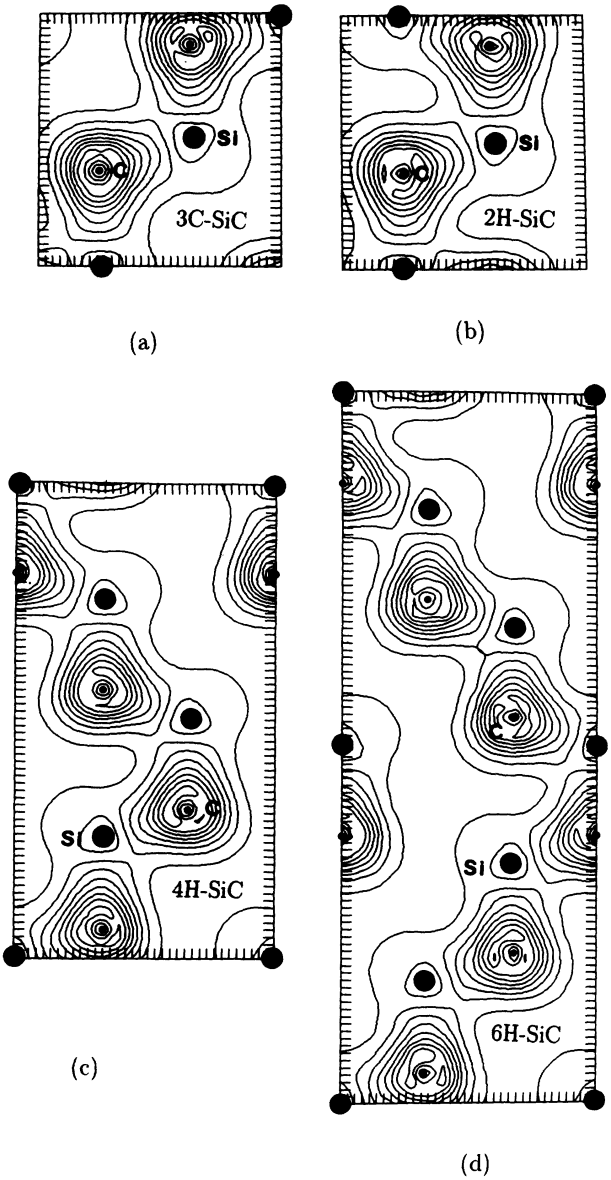

FIG. 4. Total valence charge densities in the hexagonal $(10\bar{1}0)$ planes for (a) 3*C*, (b) 2*H*, (c) 4*H*, and (d) 6*H* SiC. Small and large filled circles indicate the atomic positions of the C and Si atoms, respectively. Units are two electrons per zinc-blende cell volume with a spacing of 4.

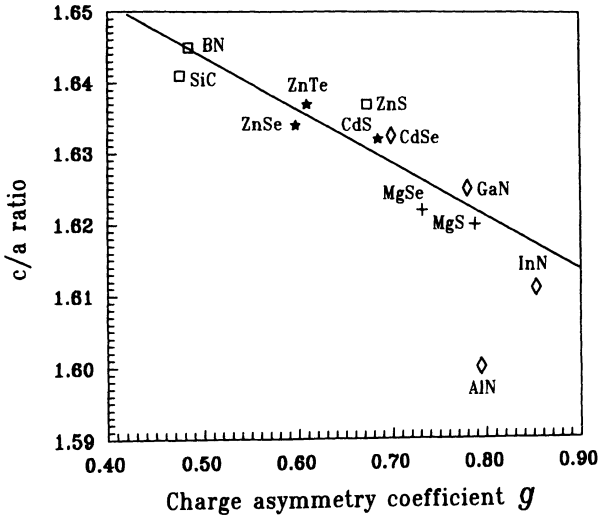

FIG. 5. Comparison of the c/a ratio with the charge-asymmetry coefficient g defined by Garcia and Cohen (Ref. 32) for several binary compounds in the wurzite structure. □: compounds showing polytypism, ★: those with the zinc-blende as well as the wurtzite structure, ◊: those with only the wurtzite structure, +: those with the NaCl as well as the wurtzite structures.

IV. ELECTRONIC STRUCTURE

The calculated energy-band structures for 3*C*, 2*H*, 4*H*, and 6*H* SiC are given in Figs. 6(a)–(d), respectively. For

comparison of the electronic structures of the 3C and 2H structures, the energy bands for 3C SiC are presented here in a nonconventional way,[35] where they are drawn at the equivalent k points in the hexagonal BZ. Since the 2H structure has a twice-larger unit cell than the cubic structure, it has twice as many bands at any k point in the hexagonal BZ. Thus, two k points in the fcc zone are mapped onto the same k point in the hexagonal zone, by folding the bands of 3C SiC as shown in Fig. 6(a). In the 4H and 6H structures, more band foldings come in because of the increase in the period of the superlattices along the hexagonal axis.

We find some similarity between the cubic and hexagonal energy bands. Similar valence-band widths are calculated of 15.33, 15.37, 15.41, and 15.49 eV for the 3C, 6H, 4H and 2H structures, respectively, showing very weakly increasing energy-band width as the hexagonal stacking nature is enhanced. In the hexagonal polytypes, the valence-band maximum states at the Γ point are split into a twofold (p_x and p_y) and a onefold (p_z) state by hexagonal crystal fields. The 2H structure has the largest band splitting of 0.137 eV, reflecting the highest hexagonal crystal field, while the 4H and 6H structures have splittings of 0.130 and 0.021 eV, respectively.

TABLE II. Electronic energy levels (E_k in eV) relative to the valence-band maximum and their pressure coefficients (dE_k/dp in meV/kbar) for 3C, 2H, 4H, SiC.

	k points	E_k	dE_k/dP
	3C		
Present	Γ_{1c}	6.30	5.11
Other[a]		6.27	5.50
Expt.[b]		6.00	
Present	X_{1c}	1.24	−0.33
Other[a]		1.21	−0.33
Expt.[b]		2.39	−0.34
Present	L_{1c}	5.37	3.92
Other[a]		5.32	3.95
Expt.[b]		4.20	
	2H		
Present	Γ_{1c}	4.86	3.66
Present	K	2.05	−0.71
Other[c]		2.76	
Expt.[b]		3.33	
Present	M	2.72	0.76
	4H		
Present	Γ_{1c}	5.18	3.70
Present	K	3.81	0.12
Present	M	2.14	0.08
Other[c]		2.89	
Expt.[b]		3.27	
	6H		
Present	Γ_{1c}	5.18	4.03
Present	K	3.41	0.29
Present	M	1.98	−0.03
Other[c]		2.92	
Expt.[b]		3.02	

[a]Reference 9 (semilocal pseudopotentials were employed).
[b]Reference 1.
[c]Reference 16 (the LMTO method was used).

Our calculated energies and their pressure derivatives for the conduction-band states are given at high symmetry points in Table II and compared with other theoretical and experimental results. All the polytypes considered in SiC are found to have indirect band gaps. However, the magnitudes of the band gaps and the energy of the minimum conduction-band states vary significantly as the percentage of hexagonal close packing increases. The 3C structure has the smallest band gap of 1.24 eV from Γ to X, while for the 2H structure, which is purely hexagonal the minimum conduction-band state occurs at the K point with a band gap of 2.05 eV. These values compare to the corresponding measured values of 2.39 and 3.33 eV.[1] The minimum conduction-band state at the X point of 3C SiC corresponds to the P_1 state which lies on the M-L axis in the hexagonal BZ, as shown in Fig. 6(a). For the 4H and 6H structures, however, band gaps of 2.14 and 1.98 eV are found at the M point, while the corresponding measured values are 3.27 and 3.02 eV.[1] Compared with experimental data, the underestimation of the band gaps ranges from 1.04 to 1.28 eV, and is known to result from the use of the LDA in our calculations. The lowest conduction-band state at the X point in the cubic structure decreases as pressure increases with a pressure coefficient of −0.33 meV/kbar with respect to the maximum valence-band state. This calculated coefficient is in good agreement with another theoretical value[9] of −0.33 meV/kbar and experimental data of −0.34 meV/kbar.[1] In the hexagonal polytypes, the M and K states in the conduction bands show different pressure behavior as the hexagonal stacking nature is enhanced; the pressure coefficient of the M state increases from a negative value to positive ones, while the K state shows the opposite behavior. Since it is generally known that the X-state energy of the cubic structure decreases with pressure due to its d-orbital character, the hexagonal crystal fields induce more d-like character for the K state. We find that the 4H and 6H structures have very small pressure coefficients of 0.08 and −0.03 meV/kbar for the M state, respectively. On the other hand, the 2H structure has a negative pressure coefficient of −0.71 meV/kbar at the K point. We plot the energy levels at high-symmetry k points as a function of the parameter describing the percentage of hexagonal close packing in Fig. 7. The variations of the energy levels in the polytypes of SiC are due to the hexagonal crystal fields. The conduction-band energies at the M and L points show similar increasing variations, while that of the K point decreases as the hexagonal-close-packing nature becomes more prominent.

The calculated densities of states (DOS) are presented for the polytypes of SiC in Fig. 8. The heights of several peaks in the DOS depend on the hexagonal stacking nature, similarly to the total energy and the energy levels. The peak near −7 eV decreases on going from the 3C to the 2H structure, while the −2-eV peak increases. The shapes of the DOS located between −16.0 and −10.0 eV are similar for the polytypes considered here, while those near the conduction-band edges are changed significantly. The hexagonal polytypes of SiC can be considered as natural superlattices. The artificial group-III-V superlattices

are characterized by band folding, band offset, and charge confinement. However, we cannot use the same arguments for the 4*H* and 6*H* SiC natural superlattices. Band offset is absent because there is no interface effect on the charge density, as shown in Fig. 4, and the stacking layer cannot be distinguished. Only the band-folding effect is important. As the band folding increases, the slope of the DOS at the conduction-band edge becomes steeper, with a maximum slope for the 6*H* structure. Compared with the cubic structure, the conduction-band state of the 6*H* structure at the P_1 point (corresponding to the *X* point in the cubic BZ) is shifted to the higher-

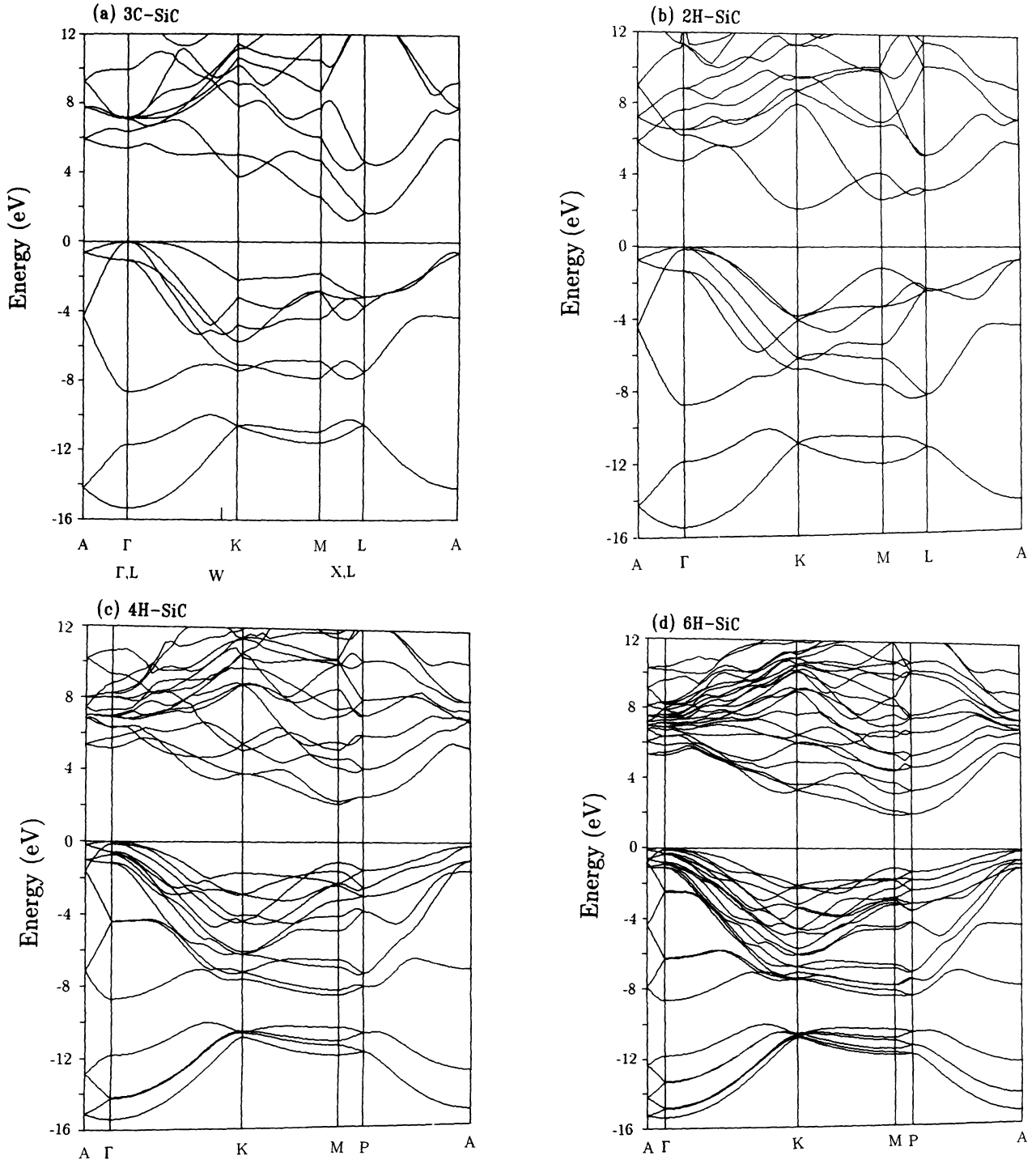

FIG. 6. Calculated energy bands for (a) 3*C*, (b) 2*H*, (c) 4*H*, and (d) 6*H* SiC. Note that the 3*C* SiC bands are presented here in a nonconventional way for direct comparison with the wurtzite bands.

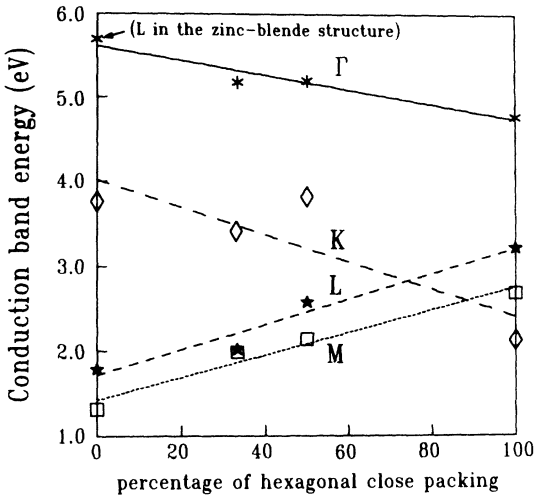

FIG. 7. Calculated electronic energy levels for the polytypes of SiC are plotted as a function of the parameter describing the percentage of hexagonal close packing.

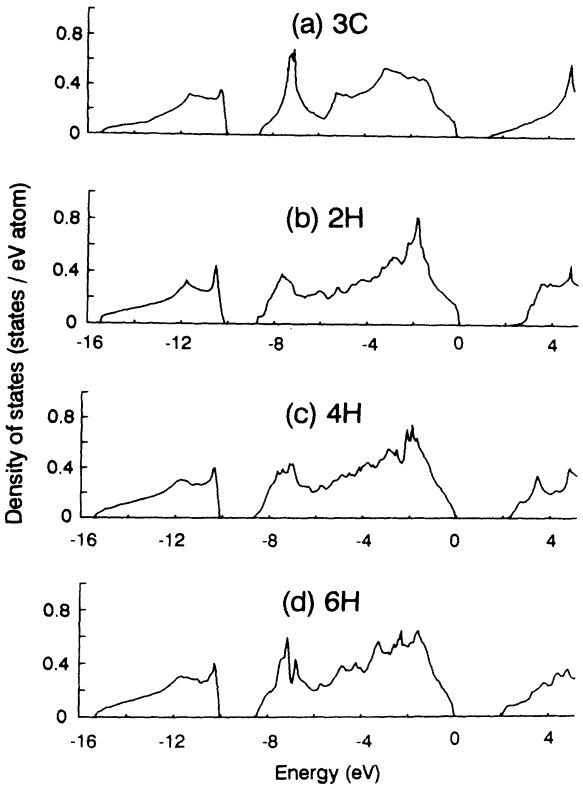

FIG. 8. Total densities of states are plotted for (a) 3*C*, (b) 2*H*, (c) 4*H*, and (d) 6*H* SiC.

energy side, while the energy at the *M* point is moved to the lower-energy region by the hexagonal crystal field. Because of this effect, the conduction-band edge states in the 6*H* structure are more or less flattened, resulting in the steepest slope in the DOS near the conduction-band edge.

V. CONCLUSIONS

We have studied the structural and electronic properties of several polytypes of SiC. The lattice constants, bulk moduli, and bulk-modulus pressure derivatives calculated for the cubic and hexagonal polytypes are found to be very similar. The charge densities are also found to be similarily distributed between the Si and C atoms, with the charge density strongly accumulated around the C atom due to the strong 2*p* potential of C, resulting in the same charge asymmetry in different polytypes. We find the polytypism of SiC to be related to the charge asymmetry because its value is on the boundary separating the zinc-blende and wurtzite structures, and the total energies of the two structures are very similar. The parameter, i.e., the hexagonality, describing the percentage of hexagonal close packing is found to be useful to understand both the ground-state properties and the electronic structures of the polytypes. As this parameter increases from cubic to hexagonal, the conduction-band minimum state changes from the *X* point to the *M* point, and then to the *K* point. This increasing-energy behavior of the *M*-conduction-band state causes flattening of the conduction-band edge states in the 6*H* structure, and thus the largest slope in the DOS is near the conduction-band edge. On the other hand, the structural stability of the hexagonal structure is maximized for the 4*H* structure because of the maximum attractive interactions between the stacking layers.

ACKNOWLEDGMENTS

This work was supported by the Korea Science and Engineering Foundation, the SPRC at Jeonbuk National University, and the CMS at Korea Advanced Institute of Science and Technology.

*Present address: NEC Research Institute, 4 Independence Way, Princeton, NJ 08540.

[1]von Münch, in *Landolt-Börnstein,* edited by O. Madelung, M. Schulz, and H. Weiss, New Series, Groups IV and III-V, Vol. 17, Pt. A (Springer, Berlin, 1982), and references therein.

[2]R. W. G. Wyckoff, *Crystal Structures* (Wiley, New York, 1963), p. 113.

[3]C. Cheong, R. J. Needs, and V. Heine, J. Phys. C **21**, 1049 (1988).

[4]J. J. A. Shaw and V. Heine, J. Phys. Condens. Matter **2**, 1049 (1988).

[5]C. Cheong, V. Heine, and I. L. Jones, J. Phys. Condens. Matter. **2**, 5097 (1990).

[6]C Cheong, V. Heine, and R. J. Needs, J. Phys. Condens. Matter **2**, 5115 (1990).

[7]P. A. Ivanov and V. E. Chelnokov, Semicond. Sci. Technol. **7**, 863, (1992).

[8]K. J. Chang and M. L. Cohen, Phys. Rev. B **35**, 8196 (1987).

[9]B. H. Cheong, K. J. Chang, and M. L. Cohen, Phys. Rev. B **44**, 1053 (1991).
[10]N. Churcher, K. Kunc, and V. Heine, J. Phys. C **19**, 4413 (1986); Solid State Commun. **56**, 177, (1985).
[11]P. J. H. Denteneer and W. van Haeringen, Phys. Rev. B **33**, 2831 (1986).
[12]P. J. H. Denteneer and W. van Haeringen, Solid State Commun. **65**, 115 (1988).
[13]W. R. L. Lambrecht, B. Segall, M. Methfessel, and M. van Schilfgaarde, Phys. Rev. B **4**, 3685 (1991).
[14]F. Bassani and M. Yoshimine, Phys. Rev. **130**, 20 (1963).
[15]C. Tuncay and M. Tomak, Phys. Status Solidi B **127**, 543 (1985).
[16]V. I. Gavrilenko, A. V. Postnikov, N. I. Klyui, and V. G. Litovchenko, Phys. Status Solidi B **162**, 477 (1990).
[17]M. L. Cohen, Int. J. Quantum Chem. **29**, 843 (1986).
[18]J. Ihm, A. Zunger, and M. L. Cohen, J. Phys. C **12**, 4409 (1979).
[19]P. Hohenberg and W. Kohn, Phys. Rev. **136**, B864 (1964); W. Kohn and L. J. Sham, *ibid.* **140**, A1133 (1965).
[20]E. Wigner, Trans. Faraday Soc. **34**, 678 (1938).
[21]N. Troullier and J. L. Martins, Solid State Commun. **74**, 613 (1990); Phys. Rev. B **43**, 1993 (1991); **43**, 8861 (1991).
[22]L. Kleinman and D. M. Bylander, Phys. Rev. Lett. **48**, 1425 (1982).
[23]C. H. Park, I.-H. Lee, and K. J. Chang, Phys. Rev. B **47**, 15996 (1993).
[24]G. Lehmann and M. Taut, Phys. Status Solidi B **54**, 409 (1972).
[25]J. Rath and A. J. Freeman, Phys. Rev. B **11**, 2109 (1975).
[26]H. Hellmann, *Einführung in die Quantenchemie* (Deuticke, Leipzig, 1937), p. 295; R. P. Feynman, Phys. Rev. **56**, 340 (1939).
[27]F. D. Murnaghan, Proc. Natl. Acad. Sci. U.S.A. **3**, 244 (1944).
[28]P. E. Van Camp, V. E. Van Doren, and J. T. Devreese, Phys. Rev. B **34**, 1314 (1986); S. Fahy, K. J. Chang, S. G. Louie, and M. L. Cohen, *ibid.* **35**, 5856 (1987).
[29]R. D. Carnahan, J. Am. Ceram. Soc. **51**, 223 (1968); E. Schreiber, N. Soga, *ibid.* **49**, 342 (1966).
[30]D. M. Ceperly and B. J. Alder, Phys. Rev. Lett. **45**, 566 (1980); J. P. Perdew and A. Zunger, Phys. Rev. B **23**, 5048 (1981).
[31]E. Holzschuh, Phys. Rev. B **28**, 7346 (1983); X. Gonze, J. P. Vigneron, and J. P. Michenaud, J. Phys. Condens. Matter **1**, 525 (1989).
[32]A. Garcia and M. L. Cohen, Phys. Rev. B **47**, 4215 (1993).
[33]J. C. Phillips, *Bonds and Bands in Semiconductors* (Academic, New York, 1973).
[34]J. R. Chelikowsky and J. C. Phillips, Phys. Rev. B **17**, 2453 (1978).
[35]M. R. Salehpour and S. Satpathy Phys. Rev. B **41**, 3048 (1990).